**Title**
Direct Evidence for the Nature of Core-Level Photoemission Satellites Using Angle-Resolved Photoemission Extended Fine Structure



**Journal**
Physical Review B, 56(24)

**Author**
Moler, Edward J.

**Publication Date**
1997-08-18

LBNL-40759
UC-410
Preprint


ERNEST ORLANDO LAWRENCE
BERKELEY NATIONAL LABORATORY

# Direct Evidence for the Nature of Core-Level Photoemission Satellites Using Angle-Resolved Photoemission Extended Fine Structure

E.J. Moler, S.A. Kellar, Z. Hussain, Y. Chen,
D.A. Shirley, W.R.A. Huff, and Z. Huang

**Accelerator and Fusion Research Division**

August 1997

Submitted to
*Physical Review B*

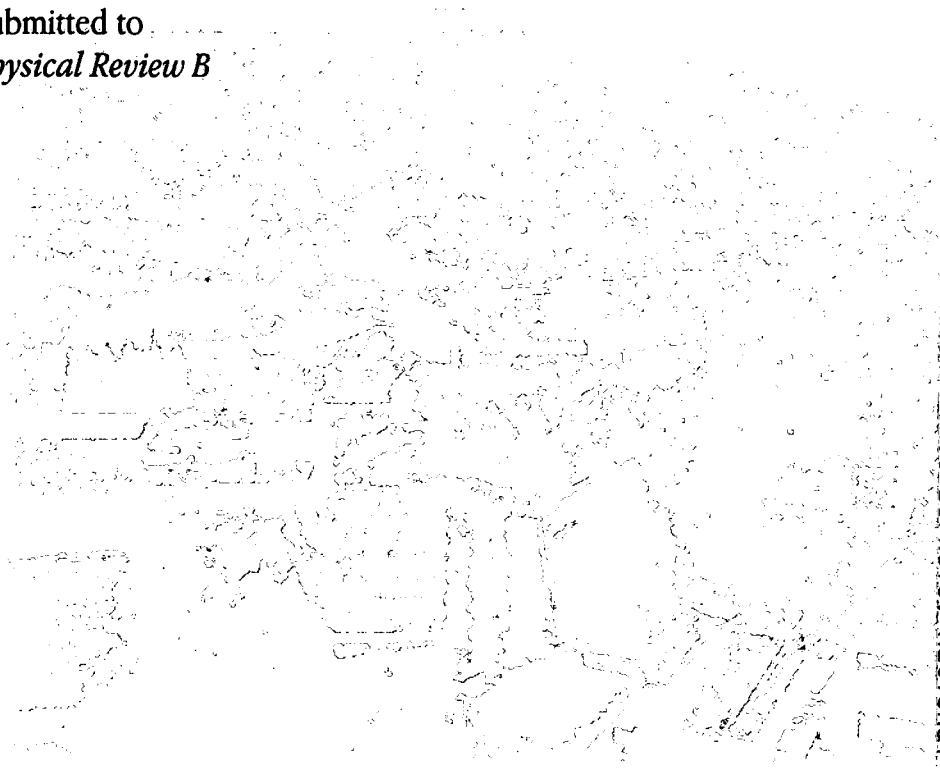

## DISCLAIMER

LBNL-40759
LSBL-410
UC-410

# Direct Evidence for the Nature of Core-Level Photoemission Satellites Using Angle-Resolved Photoemission Extended Fine Structure

E.J. Moler[a], S.A. Kellar[a], Z. Hussain[a], Y. Chen[a],
D.A. Shirley[a], W.R.A. Huff[b], Z. Huang[c]

[a]Advanced Light Source
Ernest Orlando Lawrence Berkeley National Laboratory
University of California, Berkeley, California 94720

[b]Research Center for Spectrochemistry
The University of Tokyo Photon Factory
National Laboratory for High Energy Physics
Oho 1-1, Tsukuba
Ibaraki 305, JAPAN

[c]Department of Chemistry and the James Franck Institute
The University of Chicago
Chicago, IL 60637

*This work was supported by the Director, Office of Energy Research, Office of Basic Energy Sciences, Materials Sciences Division, of the U.S. Department of Energy, under Contract No. DE-AC03-76SF00098.

# Direct Evidence for the Nature of Core Level Photoemission Satellites Using Angle-Resolved Photoemission Extended Fine Structure

Edward J. Moler, Scot A. Kellar, Zahid Hussain, Yufeng Chen, David A. Shirley

Advanced Light Source, Lawrence Berkeley National Laboratory,
1 Cyclotron Road, Berkeley, CA 94720

W. R. A. Huff
Research Center for Spectrochemistry, The University of Tokyo
Photon Factory, National Laboratory for High Energy Physics
Oho 1-1, Tsukuba
Ibaraki 305, JAPAN

Zhengqing Huang

Department of Chemistry and the James Franck Institute, The University of Chicago,
Chicago IL 60637

## Abstract

Photoemission satellites from several systems have been found to exhibit exactly the same Angle-Resolved Photoemission Extended Fine Structure (ARPEFS) as found in the main peaks, when referred to the equivalent photoelectron wavenumber k for their own photoelectrons. This provides a direct and powerful method for experimentally determining the angular momentum parameters and the intrinsic/extrinsic nature of core-level photoemission satellites. We present ARPEFS satellite data for nitrogen 1s line in c(2x2) $N_2$/Ni(100), the nickel 3p line in clean nickel (111), the carbon 1s lines in ($\sqrt{3}$x$\sqrt{3}$)R30 CO/Cu(111) and p2mg(2x1)CO/Ni(110) and the cobalt 1s line in p(1x1) Co/Cu(100). For the last two cases the "satellite" structure is actually the low-energy tail of a Doniach-Sunjic lineshape. The satellite peaks and the tails of the Doniach-Sunjic lineshapes exhibit ARPEFS curves which in all cases except one indicate angular momentum parameters identical to the main peak and an intrinsic nature.

## I. Introduction

The nature of core-level photoemission satellites from clean metal surfaces has been an active area of investigation for some time[1-13] . Satellites from molecular adsorbates on metal surfaces have been interpreted as arising from certain mechanisms and employed to study the adsorbate-substrate surface chemical bonds in a variety of systems[14-20]. Core-level satellites are generally described as arising from photoelectron transitions from the neutral ground state to "correlation states" of some type: states lying above the main hole state. Correlation states can be understood as being formed from the main hole states by correlated excitations of valence electrons into unoccupied bound states or into the continuum.

These excitations are often described as "shake-up" of the valence electrons to form a valence electron-hole pair. However, the satellite peaks in the photoelectron spectrum are produced directly by one-step photoelectron transitions no different from those to the main-peak states. The satellite is "intrinsic" in that it arises from a process which occurs largely within the source atom, leading directly to a final state with the same symmetry as the main hole state, but just lying higher in energy. Indeed, the shake-up picture, per se, while of heuristic value, is unnecessary: the main photoelectron peak and some subset of the intrinsic satellites can be regarded as being formed by transitions from the ground state to a correlated manifold of states of the same symmetry.

In this paper we present a new and rather stringent test of the above description of correlation satellites. If indeed the satellite peaks associated with core holes, and the low-energy tails accompanying photoelectron peaks in metallic systems, arise from transitions in which the photoelectron waves originate at the same source atom and are described by the same (bound and continuum) angular momenta as those of the main peak, then they should display the same diffraction phenomena.

Energy-dependent photoelectron diffraction, which we have termed angle-resolved photoemission extended fine structure (ARPEFS), to emphasize its formal similarity to EXAFS when it is observed over a large enough energy range to be analyzed by Fourier-transform methods, provides a very sensitive test of the inherent nature of intrinsic satellites[21]. The scattering phenomena underlying ARPEFS structure are implicitly dependent on the photoelectron wave originating at a precisely located source atom, on its carrying certain angular momenta, and on specific interference phenomena as it scatters from neighboring atoms and propagates to the detector. In the ideal, seemingly simplistic case that a particular satellite line in the photoelectron spectrum arises from a simple photoelectron transition to a higher-energy final state in the same correlation-state manifold as the main-line final state, the satellite's ARPEFS structure should exhibit *exactly* the same variation of intensity with energy as the main line, after correction to the same kinetic-energy scale.

In this paper we examine the ARPEFS structures of several satellite lines which we have observed in our laboratory during studies of surface systems for which the primary goal was the determination of high-accuracy[22] surface atomic structures. When we observed in the course of these studies that the satellite structures also showed ARPEFS oscillations, we elected to combine the analyses of these satellite oscillations and report them together, in this paper. In each case the satellite ARPEFS structure is compared directly with that of the main line, plotting each intensity against the actual k value of the photoelectron emitted in the process leading to the main line or the satellite structure. Thus, for a given spectrum, the satellite peak will correspond to a lower k value than that of the main peak. Section II summarizes the experimental conditions for these systems: more detailed descriptions are given (for most cases) in the publications describing the atomic surface structural determinations. Data reduction is described in Section III, and results are given and discussed in Section IV. In Section V we draw a few conclusions.

## II. Experimental

Full descriptions of the experimental conditions have been given in reports of the atomic surface structures for both CO/Cu(111)[23] and N2/Ni(100)[24]. For CO/Ni(110), experimental details were given in the structure paper[25]. The Co/Cu(100) work, which has not been published, was studied at room temperature using beam line 6-2 at the Stanford Synchrotron Radiation Laboratory (SSRL). While the exact structure was not determined, cobalt is known to grow layer-by-layer epitaxially on copper (100)[26, 27].

The CO/Cu(111) experiment was performed on beam line 9.3.2 at the Advanced Light Source (ALS) at Lawrence Berkeley National Laboratory. The $N_2$/Ni(100) experiment was performed on beam line 6.1 at SSRL. The clean nickel and CO/Ni(110) experiments were performed using beam line U3-C at the National Synchrotron Light Source at Brookhaven National Laboratory.

The samples were all cleaned and prepared using standard UHV surface-science techniques and were cooled to 80K to 120 K for the molecular adsorbates and clean nickel experiments. The x-ray angle of incidence on the sample ranged from 55° to 80° from normal and the emission direction was near-normal for all experiments. We were careful not to radiation-damage the adsorbate systems by checking the LEED pattern only briefly near the edge of the sample. It is known that the nitrogen molecule stands on end atop a nickel atom on the (100) surface[28], and the structure is known[24]. Similarly, the CO is known to occupy only atop sites in the ($\sqrt{3}$x$\sqrt{3}$)R30 structure on Cu(111), from FT-IR and EELS[29] and, most recently, ARPEFS[23]. The CO molecule in p2mg(2x1) CO/Ni(110) occupies a displaced, short-bridge site and is tilted by 19° from the surface normal[25].

## III. Data Reduction

An example x-ray photoemission (XPS) spectrum for each system is shown in Figs. 1, 2, and 3, with the experimental data points shown as circles. The best-fit curves and fitting components are also shown in Figs. 1 and 3. These fits were used to extract the peak intensities for the ARPEFS curves. The range of integration for each spectrum in Fig. 2 is marked by vertical solid lines. The integrated intensities above the background in these regions were used to construct the ARPEFS curves, shown on the right. The abscissa in this plot is the electron wave-number k, in $Å^{-1}$, for each peak.

The main N 1s XPS peak is known to consist of two components, each associated with the nitrogen closer or farther from the nickel surface[17]. We have summed them to get a sum ARPEFS curve. The nickel $3p_{1/2}$ and $3p_{3/2}$ peaks were similarly summed. The C 1s XPS peak in p2mg(2x1)CO/Ni(110) has been shown to have a Doniach-Sunjic (DS) line shape[25, 30]. The cobalt 1s peak in p(1x1) Co/Cu(100) also shows the Doniach-Sunjic line shape. We have extracted the intensities for these spectra by integrating the area above the background across two regions, one centered on the peak and the other at 10 eV lower kinetic energy, as shown with vertical lines. It is clear from the figures that the satellite peaks exhibit the same ARPEFS diffraction pattern as the main peak, with the exception of the nickel 13 eV satellite, which will be discussed further below. The ARPEFS curves for the p2mg(2x1)CO/Ni(110) and p(1x1) Co/Cu(100) systems have been Fourier-smoothed to 10 Å to aid comparison.

## IV. Results and Discussion

Two important conclusions, which are related but separate, can be drawn from the similarities between the main- and the satellite-peak ARPEFS curves. The first is that these satellite peaks and the Doniach-Sunjic tails in the photoemission spectrum must arise from "intrinsic" energy-loss mechanisms: i.e., intrinsic in the photoemission process from the initial atomic core-electron state (as opposed, for example, to energy losses through inelastic processes extrinsic to the source atom) . This conclusion stems from the extreme sensitivity of ARPEFS to the position of the outgoing electron wave's origin, which is ca. 0.01 Å. The oscillatory ARPEFS structure in a satellite line must itself arise from interference between an unscattered outgoing wave which propagates toward the detector and an elastically scattered wave at the same kinetic energy (and k value) which scatters off neighboring atoms and then propagates toward the detector. An inelastic scattering channel would not interfere with the unscattered outgoing wave to produce an ARPEFS structure. Photoemission from a delocalized valence orbital which is not centered on an ion core would most likely lead to an outgoing electron wave that would exhibit a very different diffraction pattern.

The phenomenon of the "satellite" area of the photoemission spectrum showing ARPEFS interference structure exactly the same as that of the "main" peak can be easily understood by regarding the photoemission process as leading to eigenstates of the Hamiltonian for the core-hole manifold which are reached directly in a one-step process: the overlap of the final states and the initial ground state (exclusive of the photoemitted electron) will essentially determine the intensity spectrum for the photoemission process. Whether the spectral intensity below the main peak is discrete, as in the molecular adsorbate systems and nickel, or continuous, as in the DS lineshape case, the same general one-step picture applies.

The fact that we find these peaks to be intrinsic is compatible with the interpretation of Tillborg, Nilsson, and Martensson that the molecular adsorbate satellites

are due to "shake-up" channels which originate from a single-step process[15]. This heuristic interpretation considers the final state of the remaining electrons to be strongly influenced by the newly created core-hole. This state is not an eigenstate of the unperturbed system, leading to a final state which is a sum of the new eigenstates of the adsorbate-plus-core-hole system and thus has significant probability of valence excitations. The nickel 6 eV satellite is also intrinsic. This is consistent with the current understanding of its origin as being due to an excitation of a single d-level electron correlated with the 3p core excitation into the continuum, leaving a $3d^9$ valence configuration in the final state[4]. The DS line shape is also derived assuming an intrinsic excitation of the Fermi sea in the core-hole creation process. Our results also confirm the intrinsic origin of the DS tail. We note the relation between our results and those of Osterwalder, et. al.[12] who found that the plasmon-loss peaks of the aluminum 2s core-level show electron scattering effects at high kinetic energies (1136 eV). At high kinetic energies, the scattering effects are dominated by forward scattering and kikuchi processes, in contrast to the energy regime of our work which is dominated by multiple-scattering effects and back-scattering.

The second conclusion which can be drawn from the similarities in the ARPEFS curves is that the transitions leading to the satellite peaks have the same values for the angular momentum variables as do those for the main peak. The dipole selection rules of photoemission are known to be valid for the main peaks and have been used successfully to model the diffraction curves for many systems. Because different angular momenta in the free-electron final state of the photoelectron lead to different and characteristic diffraction curves[22], the similarity of the ARPEFS curves indicates that those angular momenta and, by implication, also the angular momenta of the bound, final satellite states, are the same as the angular momenta characterizing the main-peak transition.

Expressing this conclusion in the terminology often associated with discussions of satellite excitations, the valence excitations are thereby restricted to "monopole" excitations for single electrons and to a net zero angular momentum change for two-electron excitations

in these systems. This agrees well with previous theoretical investigations into the 6 eV nickel satellite where a d-d transition is considered the most likely origin of that satellite structure[4]. It has been suggested that there may be excitations to s and d-like Rydberg states in the carbon 1s XPS of c(2x2) CO/Ni(100)[15]. However, for the similar CO/Cu(111) system, it is apparent from our data that there is essentially no angular momentum transfer and that the transitions to np states dominate.

Finally, we address the apparent difference in the nickel 13 eV satellite from the main and 6 eV peaks (see Figs. 3, 4 and 5). This peak has been attributed to the excitation of two d-band electrons at the 3p resonance energy, leaving a $3d^8$ configuration in the final state[2]. In Fig. 4a we show the Fourier transform (FT) spectrum of the three nickel ARPEFS curves, normalized to the same intensity in the first peak. Each FT exhibits peaks at the same near-neighbor path length differences, except the 13 eV satellite peak, which shows significantly less intensity above ~ 3Å. It is not apparent from the FT whether or not the phase of the 13 eV curve matches that of the others, so we also show in Fig. 4b the ARPEFS curves which have been Fourier filtered to 3 Å, including only the 2 Å peak. It has been shown previously that odd-parity final states will give ARPEFS curves which are 180° out of phase with even-parity final states[22]. From the filtered curves it is apparent that the final states are of the same parity.

The angular momentum of the 13 eV satellite final state may be either d-like or s-like. The main peak is mostly d-like, in accordance with the atomic radial matrix elements (RME) for nickel[29]. We have performed ARPEFS calculations using both an s-wave final state and the d-like published atomic RME[31]. The results of these calculations are shown in figure 5a. While the d-like RME calculation matches the main-peak ARPEFS curve very well, the s-wave curve does not. The 13-eV satellite curve does not match either calculation. The FT of the calculated and the satellite ARPEFS curves are shown in Fig. 5b. Comparison of the satellite peak FT with the two calculations lead us to conclude that the satellite peak is predominately d-like in the final state.

We can only speculate on the suppressed intensity of oscillations of the 13 eV satellite at longer path lengths. These peaks are due to scattering from atoms more distant from the emitter than the first peak. One possible explanation is that the core hole in the presence of the $3d^8$ configuration has a significantly shorter lifetime than the core hole with a $3d^{10}$ or $3d^9$ final state. This would result in a shorter coherence length of the outgoing electron wave, damping the intensity oscillations for more distant scatterers. Further theoretical investigation of the Auger decay mechanisms of the excited state would be needed to evaluate this possibility. We also considered the possibility of the peak being in some way associated with the surface of the metal. However, ARPEFS curves calculated using only the surface layer of atoms as photoemitters do not differ significantly from those of the bulk with many layers of emitters.

## V. Conclusion

We have shown for the first time that photoemission satellite peaks from multi-electron excitations exhibit an ARPEFS diffraction pattern. Examination of this pattern leads to unique information on the angular momentum and intrinsic/extrinsic nature of the satellite. We find that the core level satellite peaks of carbon 1s from $(\sqrt{3}x\sqrt{3})R30$ CO/Cu(111), nitrogen 1s from c(2x2) $N_2$/Ni(100), and nickel 3p from clean nickel(111) are all intrinsic peaks with final state angular momenta identical to those for the main peaks, as dictated by the photoemission selection rules. Similarly, the tail of the Doniach-Sunjic line shapes in cobalt 1s from p(1x1) Co/Cu(100) and carbon 1s from p2mg(2x1) CO/Ni(110) also originate from intrinsic processes and have final state angular momenta identical to those for the maximum (main) peak.

## Acknowledgments

We thank the staff and management of the Advanced Light Source at Lawrence Berkeley National Laboratory, the National Synchrotron Light Source and Brookhaven National Laboratory, and the Stanford Synchrotron Radiation Facility for their assistance and support with the experimental work. We also thank L. J. Terminello, L. Wang, X. Zhang, and S. Kim for their assistance with the experimental work. This work was supported by the Director, Office of Energy Research, Office of Basic Energy Sciences, Chemical Sciences Division of the U. S. Department of Energy under contract No. DE-AC03-76SF00098.

## References


1 S. Hüfner, J. Osterwalder, T. Greber, and L. Schlapbach, Physical Review B **42**, 7350 (1990).

2 O. Bjorneholm, J. N. Andersen, C. Wigren, and A. Nilsson, Physical Review B **41**, 10408 (1990).

3 L. C. Davis and L. A. Feldkamp, Physical Review Letters **44**, 673 (1980).

4 W. Eberhardt and E. W. Plummer, Physical Review B **21**, 3245 (1980).

5 M. Iwan, F. J. Himpsel, and D. E. Eastman, Physical Review Letters **43**, 1829 (1979).

6 B. W. Jepsen, F. J. Himpsel, and D. E. Eastman, Physical Review B **26**, 4039 (1982).

7 Y. Liu, Z. Xu, and P. D. Johnson, Physical Review B **52**, R8593 (1995).

8 N. Martensson and B. Johansson, Physical Review Letters **45**, 482 (1980).

9 N. Martensson, R. Nyholm, and B. Johansson, Physical Review B **30**, 2245 (1984).

10 G. van der Laan, M. Surman, M. A. Hoyland, C. F. J. Flipse, B. T. Thole, U. Seino, H. Ogasawara, and A. Kotani, Physical Review B **46**, 9336 (1992).

11 M. F. Lopez, A. Gutierrez, C. Laubschat, and G. Kaindl, Solid State Communications **94**, 673 (1995).

12 J. Osterwalder, T. Greber, S. Hüfner, and L. Schlapbach, Physical Review B **41**, 12495 (1990).

13 W. F. Egelhoff, Physical Review B **30**, 1052 (1984).

14 H. Ueba, Physical Review B **45**, 3755 (1992).

15 H. Tillborg, A. Nilsson, and N. Martensson, Journal of Electron Spectroscopy and Related Phenomena **62**, 73 (1993).

16 D. Lovric and B. Gumhalter, Surface Science **278**, 108 (1992).

17 A. Nilsson, H. Tillborg, and N. Martensson, Physical Review Letters **67**, 1015 (1991).

18 A. Nilsson, Ph. D. Thesis, Department of Physics, *Core Level Electron Spectroscopy Studies of Surfaces and Adsorbates*, Uppsala University at Uppsala, Sweden, 1989.

19 J. Schirmer, G. Angonoa, S. Svensson, D. Nordfors, and U. Gelius, Journal of Physics B: Atomic and Molecular Physics **20**, 6031 (1987).

20 J. C. Fuggle, E. Umbach, D. Menzel, K. Wnadelt, and C. R. Brundle, Solid State Communications **27**, 63 (1978).

21 J. J. Barton, C. C. Bahr, C. C. Robey, Z. Hussain, E. Umbach, and D. A. Shirley, Physical Review B **34**, 3807 (1986).

22 W. R. A. Huff, Y. Zheng, Z. Hussain, and D. A. Shirley, Journal of Physical Chemistry **98**, 9182 (1994).

23 E. J. Moler, W. R. A. Huff, S. A. Kellar, Y. Zheng, E. A. Hudson, Z. Hussain, Y. Chen, and D. A. Shirley, Physical Review B **54**, 10862 (1996).

24 E. J. Moler, W. R. A. Huff, S. A. Kellar, Z. Hussain, Y. Chen, and D. A. Shirley, Chemical Physics Letters **264**, 504 (1997).

25 Z. Huang, Z. Hussain, W. R. A. Huff, E. J. Moler, and D. A. Shirley, Physical Review B **48**, 1696 (1993).

26 J. A. C. Bland, D. Pescia, and R. F. Willis, Physical Review Letters **58**, 1244 (1987).

27 A. Clarke, G. Jennings, R. F. Willis, and P. J. Rous, Surface Science **187**, 327 (1987).

28 J. Stohr and R. Jaeger, Physical Review B **26**, 4111 (1982).

29 R. Raval, S. F. Parker, M. E. Pemble, P. Hollins, J. Pritchard, and M. A. Chesters, Surface Science **203**, 353 (1988).

30 S. Doniach and M. Sunjic, Journal of Physics C: Solid State Physics **3**, 285 (1970).

31 S. M. Goldberg, C. S. Fadley, and S. Kono, Journal of Electron Spectroscopy and Related Phenomena **21**, 1981 (1981).

## Figure Captions

### Figure 1.

XPS spectra and ARPEFS chi curves for a) ($\sqrt{3}$ x $\sqrt{3}$)R30° CO/Cu(111) of the carbon 1s, and b) c(2 x 2) $N_2$/Ni(100) of the N 1s core-level. The circles in the XPS spectra (left) represent experimental data and the solid curve is the best fit using the components shown in dashes. The peaks were fitted with Voigt functions to extract their intensities. The ARPEFS curve for each peak is shown on the right. Each curve is plotted against the k-value of the photoelectron associated with its corresponding peak. The two main peaks in (b) are summed and the k-value used for plotting the ARPEFS curve is the mean of the two.

### Figure 2.

XPS and ARPEFS curves of a) p2mg(2 x1 ) CO/Ni(110), of the carbon 1s core-level, and b) p(1x1) Co/Cu(100) of the cobalt 1s. The circles in the XPS spectra (left) represent data and the dashes indicate the background component of the spectra. The peak and tail intensities were extracted by numerical integration within the ramges indicated by solid, vertical lines in the XPS spectra. The ARPEFS curves (right) are plotted against the wave-number k of the center of the corresponding integration region.

**Figure 3.**

Clean Ni(111) XPS spectrum (left) and normal emission ARPEFS (right). The circles in the XPS spectrum represent experimental data and the solid curve is the best fit using the components shown in dashes. The peaks were fitted with Voigt functions to extract their intensities. The main peak ARPEFS curve was derived from the sum of the 3P 1/2 and 3/2 peak intensities, and it is plotted against the mean of the two main peak positions. The 13 eV satellite curve intensity has been scaled by x5.

**Figure 4.**

(a) The Fourier transform of the nickel ARPEFS curves. (b) The ARPEFS curves, Fourier-filtered with a 3 Å cutoff to examine the phase of the dominant component. All of the 13 eV satellite curves were scaled by x5 .

**Figure 5.**

Comparison of the 13 eV satellite ARPEFS curve from clean Ni(111) with d-like and s-like final-state multiple-scattering calculations and their Fourier transforms.

(a) C 1s from ($\sqrt{3}$ x $\sqrt{3}$ )R30° CO/Cu(111)

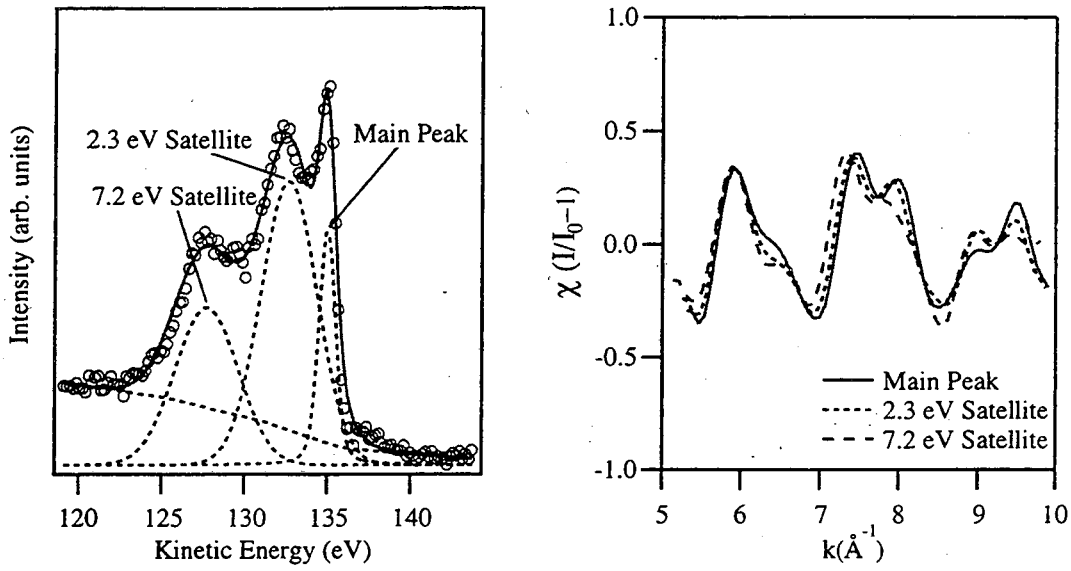


(b) N 1s from c(2 x 2) $N_2$/Ni(100)

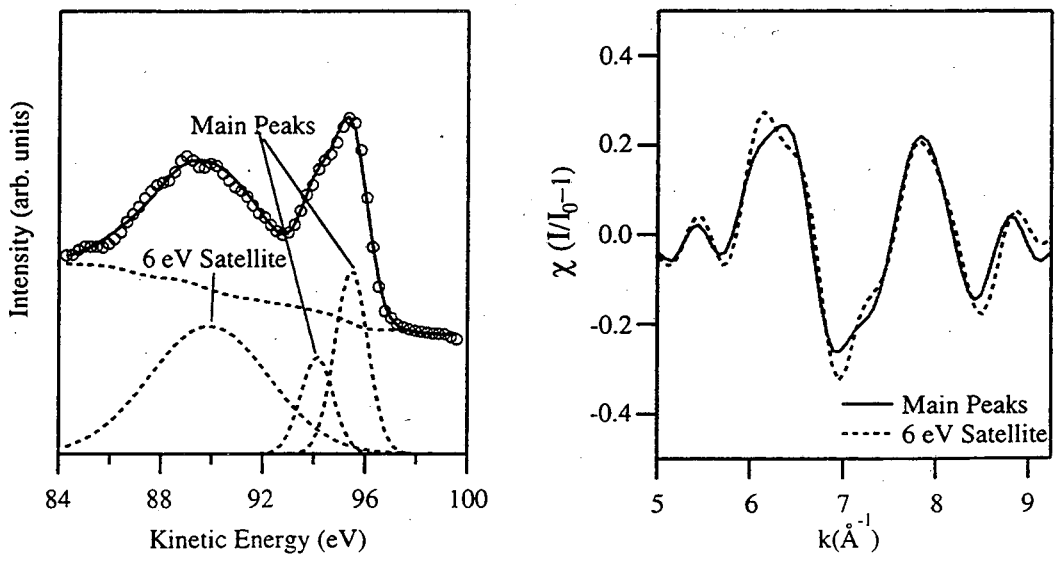


Figure 1.

(a) C 1s from p2mg(2x1) CO/Ni(110)

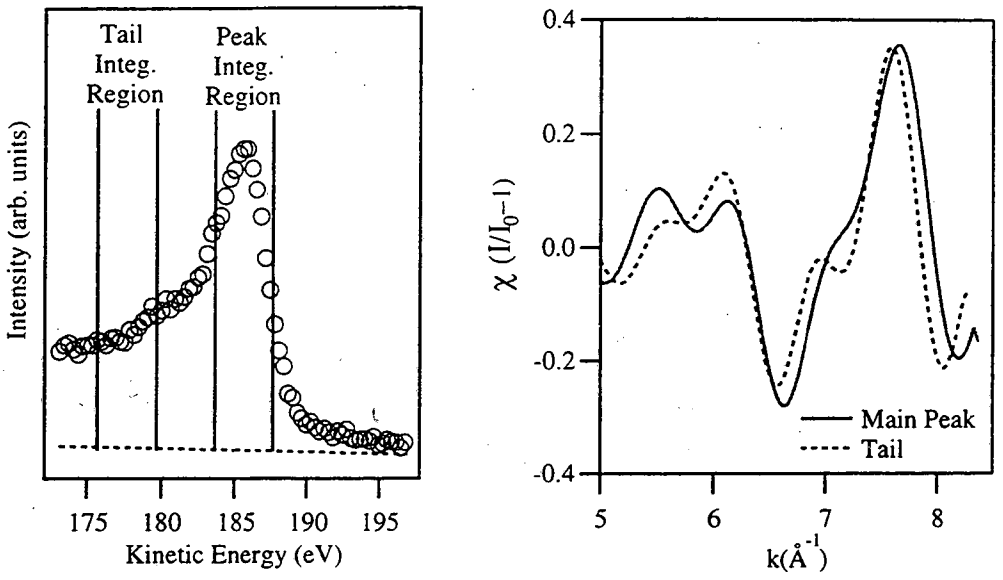


(b) Co 1s from p(1x1) Co/Cu(100)

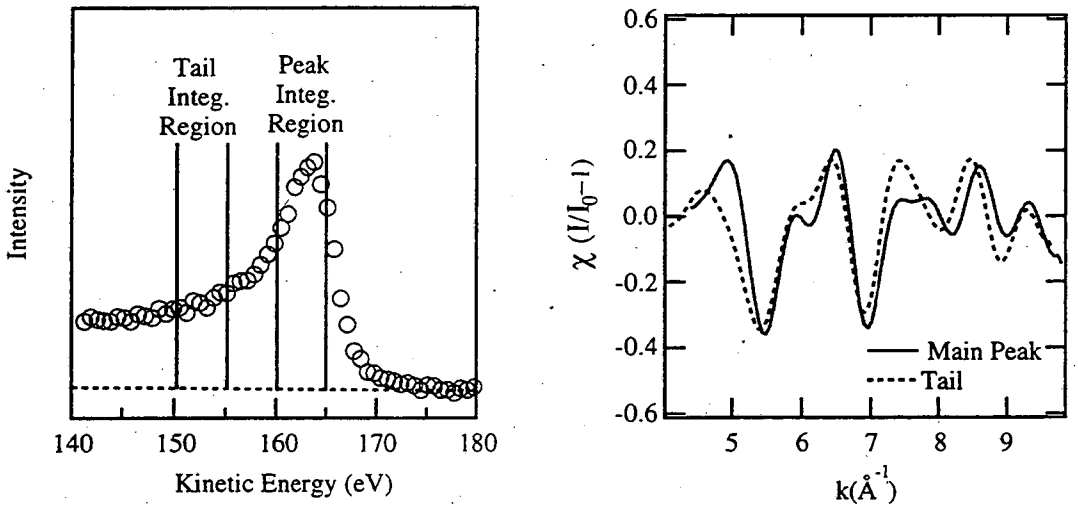


Figure 2.

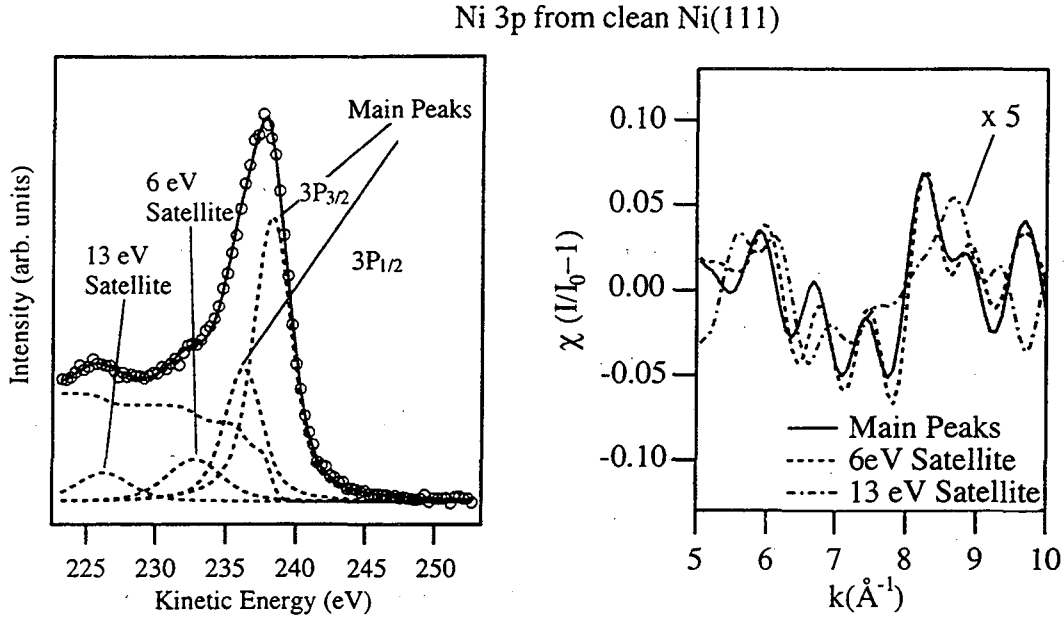
Ni 3p from clean Ni(111)
Main Peaks
6 eV
Satellite
3P3/2
13 eV
Satellite
3P1/2
Intensity (arb. units)
225
230
235
240
245
250
Kinetic Energy (eV)
0.10
0.05
0.00
-0.05
-0.10
χ (I/I0−1)
x 5
Main Peaks
6eV Satellite
13 eV Satellite
5
6
7
8
9
10
k(Å-1)

Figure 3.

(a)

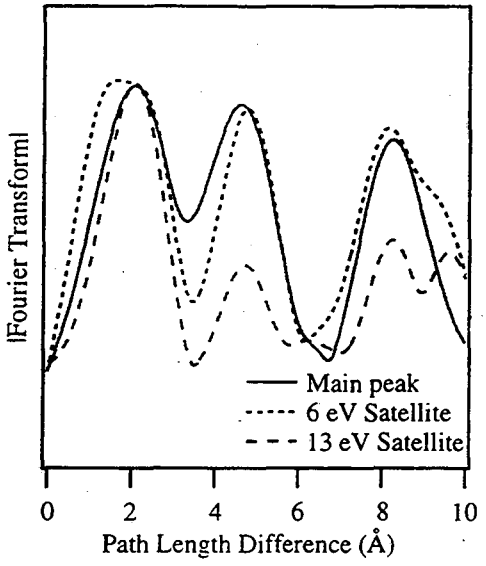
|Fourier Transform|
Main peak
6 eV Satellite
13 eV Satellite
0
2
4
6
8
10
Path Length Difference (Å)

(b)

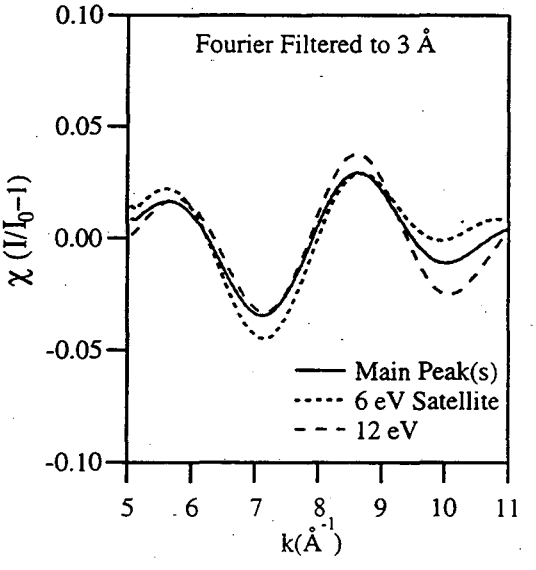
Fourier Filtered to 3 Å
0.10
0.05
0.00
-0.05
-0.10
χ (I/I0−1)
Main Peak(s)
6 eV Satellite
12 eV
5
6
7
8
9
10
11
k(Å-1)

Figure 4.

(a)

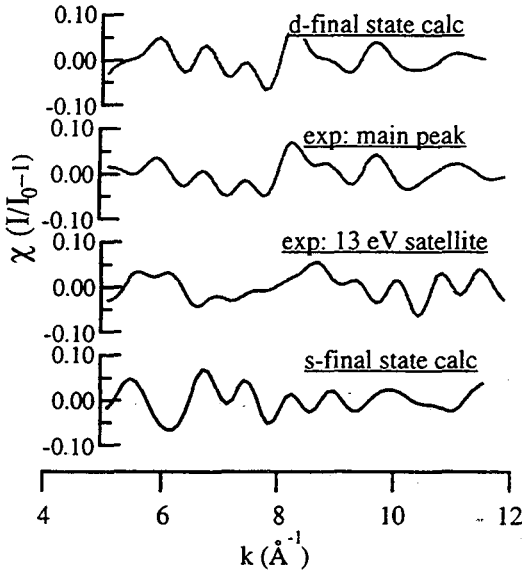
0.10
0.00
-0.10
d-final state calc
exp: main peak
exp: 13 eV satellite
s-final state calc
χ (I/I0−1)
4
6
8
10
12
k (Å-1)

(b)

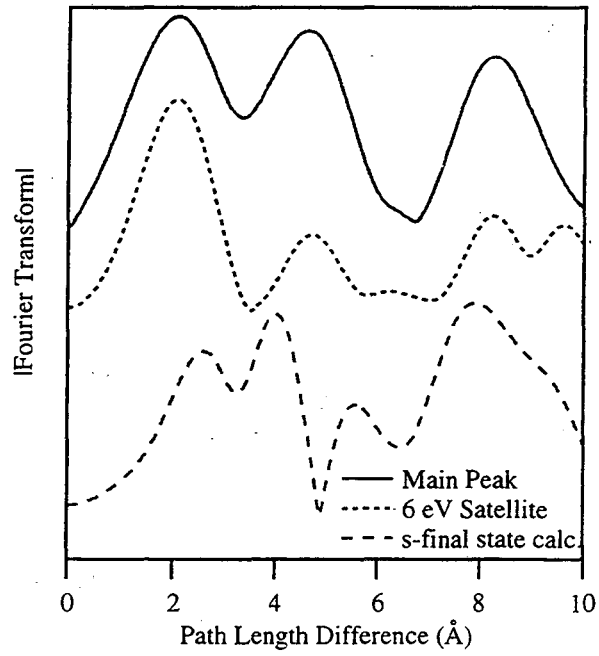
|Fourier Transform|
Main Peak
6 eV Satellite
s-final state calc
0
2
4
6
8
10
Path Length Difference (Å)

Figure 5.

Ernest Orlando Lawrence Berkeley National Laboratory
One Cyclotron Road | Berkeley, California 94720

Prepared for the U.S. Department of Energy under Contract No. DE-AC03-76SF00098